PHYSICAL REVIEW B VOLUME 52, NUMBER 18 1 NOVEMBER 1995-II

Phase-transition sequence of Rb_2ZnCl_4 obtained by study of internal vibrational modes

I. Noiret, Y. Guinet, and A. Hedoux

Laboratoire de Dynamique et Structure des Matériaux Moléculaires, Unité Fondamentale de Recherche de Physique, URA 801, Université de Lille 1, Bâtiment P5, 59655 Villeneuve D'Ascq, France

(Received 10 January 1995; revised manuscript received 10 July 1995)

Raman-scattering experiments have been performed to study the successive phase transitions of Rb_2ZnCl_4 over the temperature range 15–400 K in the Zn-Cl stretching mode region. The observation of extra Raman lines, not predicted by group theory in the normal phase, reveals that Rb_2ZnCl_4 possesses an orientational disorder of the chlorozincate groups. At low temperature, Raman-scattering spectra clearly exhibit two phase transitions at 80 and 50 K. These ones are strongly correlated with the disorder observed in the normal phase.

I. INTRODUCTION

The numerous studies that have been carried out on Rb_2ZnCl_4 crystals have shown that this compound can be found in at least four phases depending on temperature.[1] The present paper reports a thorough Raman-scattering investigation of the stretching modes over these four phases, the main characteristics of which are displayed in Table I.

The highest-temperature phase transition of Rb_2ZnCl_4 is the normal (N)-incommensurate (*INC*) phase transition[10] at 302 K (T_I). For a long time, the only assumed model for this transition was a purely displacive one involving an hypothetical soft mode as it was observed in K_2SeO_4.[11] This interpretation seemed to be supported by the identification of the amplitude mode[8,12] in the *INC* phase, by the interpretation of nuclear-magnetic-resonance experiments[13,14] and also by the observation of elastic anomalies in sound velocity measurements[15] around T_I. Hirotsu, Toyota, and Hamano[15] interpreted the softening of the acoustic c_{44} mode in terms of a bilinear interaction between this mode and the optic B_{3g} mode at the Brillouin-zone center (Γ point). However one must notice that no soft mode has been as yet observed in the N phase of Rb_2ZnCl_4. A very careful research for such a mode in the isostructural Rb_2ZnBr_4 compound has even given negative results.[16]

In 1983, by analogy with the case of Rb_2ZnBr_4 (Ref. 17) and $(NH_4)_2ZnCl_4$,[18] where substantial disorders had been found in the N phase, Itoh *et al.*[19] analyzed their x-ray-diffraction experiments on the N paraelectric phase of Rb_2ZnCl_4 in the frame of a model assuming orientationally disordered $ZnCl_4$ groups. This led to a better fitting of their data (especially more reasonable thermal amplitudes) than using a model with ordered tetrahedra. The first purpose of the present study of the stretching modes via Raman scattering is to get better insight into a similar disorder occurring in the N phase of Rb_2ZnCl_4.

The *INC* phase, characterized by satellite lines depending on temperature, has been investigated via neutron scattering[20,21] and x-ray diffraction.[22,23] The modulation $\vec{q}_\delta=[1/3-\delta(T)]\vec{c}^*$ has been principally described in terms of $(0,Ry,Rz)$ rotations of the $ZnCl_4^{2-}$ tetrahedra, considered as rigid bodies, and of $(Tx,0,0)$ translations of Rb^+ ions[24] in the $P(Pmcn{:}ss\bar{1})$ super space group. At lower temperature, the modulation wave vector locks into the rational value 1/3 along $\vec{c}^*$ and generates a commensurate (C) ferroelectric phase at $T_L=189$ K. The *INC-C* phase transition is characterized by a thermal hysteresis relating to "physical quantities" such as the modulation wave vector,[25,26] the birefringence,[27] and the dielectric constant.[28,29] The second

TABLE I. Phase transition sequence of Rb_2ZnCl_4.

Transition temperature		T_1 75 K		T_L 189 K		T_I 302 K	
Phase	IV		III		II		I
	Ferroelectric (Refs. 2,3) Commensurate		Ferroelectric (Ref. 4) Commensurate		*INC* (Refs. 5–7)		Paraelectric Normal
Space group	$C1c1$ Monoclinic		$P(P2_1cn{:}\bar{1}s\bar{1})$ Orthorhombic		$P(Pmcn{:}ss\bar{1})$ Orthorhombic		$Pmcn$ Orthorhombic (Refs. 8,9)
Lattice parameters			$a'=3a$ $b'=b$ $c'=c$				$a=7.285$ Å $b=12.730$ Å $c=9.265$ Å
Wave vector			$\vec{q}=(1/3)\vec{c}^*$		$\vec{q}_\delta=[1-\delta(T)](1/3)\vec{c}^*$		
Molecules per unit cell	$Z=24$?		$Z=12$				$Z=4$

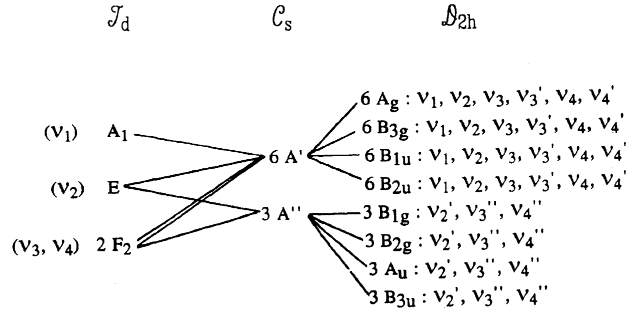

FIG. 1. The correlation between the free ion tetrahedral symmetry $\mathcal{T}_d$ and the symmetry of the N phase $\mathcal{D}_{2h}$ through the site symmetry $\mathcal{C}_s$.

purpose of this study is to analyze the behavior of the modulation in the successive phases of Rb_2ZnCl_4 through Zn-Cl stretching mode study.

Still lower, around 75 K, anomalies in dielectric constant and birefringence measurements suggest a ferroelastic second-order phase transition[30] leading to a monoclinic lattice with space group $C1c1$.[31] Our third and last purpose is to determine the phase transition sequence at low temperature of Rb_2ZnCl_4.

II. EXPERIMENTAL PROCEDURE

The Raman-scattering experiments were carried out using single crystals of Rb_2ZnCl_4 grown by slow evaporation of RbCl and $ZnCl_2$ aqueous solution at room temperature. They were performed over a range of temperature extending from 15 to 400 K. Two different methods had to be used to cover this range. Temperatures higher than 300 K were attained directly heating the crystal by a compressed hot air stream system. Raman-scattering spectra were thus recorded at different temperatures by step of 15 K from 300 up to 400 K. The lowest temperatures down to 15 K were reached using a closed-cycle cryostat developed in the laboratory and described in an earlier paper.[32] The sample was progressively cooled to record spectra about every 10 K down to 15 K.

In all the Raman-scattering experiments, the sample was excited with the 4800 Å radiation of the Ar^+ laser. The scattered light was analyzed by a CODERG T800 triple monochromator with a spectral resolution of 1 cm^{-1}. A photon Counter 1109 of Princeton Applied Research and a Dilor data acquisition system were used to record the spectra. Frequencies and halfwidths of the observed bands were determined by fitting these spectra using damped oscillator profiles.

TABLE II. Irreducible representations for the $ZnCl_4$ tetrahedra internal modes in the different symmetries.

Frequency	Tetrahedral symmetry	Site symmetry	Crystal symmetry
	$\mathcal{T}_d$	$\mathcal{C}_s$	$\mathcal{D}_{2h}$
(275 cm^{-1}) ν_1	A_1	A'	$A_g \oplus B_{3g}$
(79 cm^{-1}) ν_2	E	$A' \oplus A''$	$A_g \oplus B_{1g} \oplus B_{2g} \oplus B_{3g}$
(306, 104 cm^{-1}) ν_3, ν_4	F_2	$2A' \oplus A''$	$2A_g \oplus B_{1g} \oplus B_{2g} \oplus 2B_{3g}$

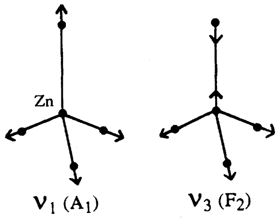

FIG. 2. ν_1 symmetrical stretching mode and ν_3 antisymmetrical stretching mode of the $ZnCl_4$ tetrahedra.

The Raman scattering spectra of Rb_2ZnCl_4 were measured in the 250–350 cm^{-1} frequency region for different temperatures and different light polarizations. It seems that the second-order effects in the A_2ZnCl_4 (A=Rb,K . . .) compounds are negligible so the modes in this region (the tetrahedron internal stretching modes) are not significantly coupled to external phonons. No peaks with frequency shifts larger than 400 cm^{-1} were observed.[33] In the following, Porto's notation is used to specify the geometry and the polarizations of an experiment. For each studied temperature, the A_g, B_{1g}, B_{2g}, and B_{3g} Raman-scattering spectra were recorded in $c(aa)b$, $c(ba)b$, $c(ac)b$, and $c(bc)b$ geometries, respectively.

III. GROUP THEORY BACKGROUND

The deconvolution of the Raman-scattering spectra leads to three types of information: intensity shifts, frequency shifts, and linewidth shifts. In order to exploit these data it is useful to determine which are the possible modes that occur in Rb_2ZnCl_4 crystals for the four configurations studied here. The observed spectra contain components due to the internal vibrations of zincate ions $ZnCl_4^{2-}$ and due to the phonon modes. The internal modes for the unit-cell symmetry appear as the result of the coupling between the free radical symmetry and the site symmetry.

Above room temperature, Rb_2ZnCl_4 is in the N phase and belongs to the $Pmcn$ space group. The correlation between the free ion tetrahedral symmetry ($\mathcal{T}_d$) and the crystal symmetry in the paraelectric phase ($\mathcal{D}_{2h}$) through the site symmetry $\mathcal{C}_s$ is given in Fig. 1. If we consider the stretching modes only (the ν_1 and ν_3 modes of the free ion), the symmetry of these 16 modes are as follows:

$$\Gamma \cdot \equiv \cdot 3A_g \oplus 3B_{3g} \oplus B_{1g} \oplus B_{2g} \oplus A_u \oplus B_{3u} \oplus 3B_{1u} \oplus 3B_{2u} ,$$

where only the eight gerade modes are Raman active.

The results are summed up in Table II. Since there are four molecules per unit cell, the two stretching modes of the tetrahedra provide a total of eight stretching modes in the crystal through Davydov splitting:[34] three for each of the A_g and B_{3g} symmetries (ν_1, ν_3, and ν_3') and one for each of the B_{1g} and B_{2g} symmetries (ν_3'') (Fig. 2).

In the INC phase the first-order satellites are observed in x-ray diffraction[22,35] or in neutron scattering.[36,37] Thus the modulation can be considered as essentially sinusoidal at temperatures above the soliton regime and in the quadridimensional formalism only the terms $l=0$ and $l=\pm1$ are expected to occur significantly, the other contributions being

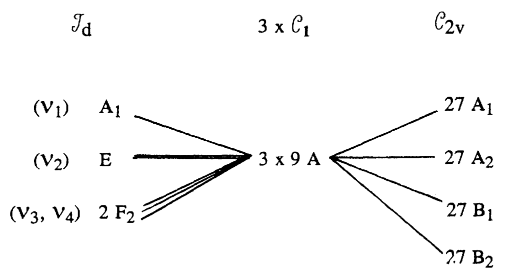

FIG. 3. The correlation between the free ion tetrahedral symmetry $\mathscr{T}_d$ and the symmetry of the C phase $\mathscr{C}_{2v}$ through the site symmetry $\mathscr{C}_1$.

negligibly small. Accordingly the irreducible representations active in Raman scattering are[38]

$$\Gamma \cdot \equiv \cdot 12A_g \oplus 15B_{1g} \oplus 15B_{2g} \oplus 12B_{3g}.$$

Below 192 K, Rb_2ZnCl_4 is in the C phase ($P2_1cn$ symmetry). The correlation between the free ion tetrahedral symmetry ($\mathscr{T}_d$) and the symmetry of the C phase ($\mathscr{C}_{2v}$) through the site symmetry $\mathscr{C}_1$ is given in Fig. 3. It can be noticed that, if one considers the stretching modes only (ν_1 and ν_3 modes), 12 modes are found to occur for each irreducible representation of the $\mathscr{C}_{2v}$ group:

$$\Gamma \cdot \equiv \cdot 12A_1 \oplus 12A_2 \oplus 12B_1 \oplus 12B_2.$$

IV. ORIENTATIONAL DISORDER IN THE NORMAL PHASE

A. Stretching mode analysis

The stretching mode analysis in the N phase for the four studied scattering orientations led to a fairly complete assignment of the modes. Let us first consider the $c(aa)b$ (A_g symmetry) and the $c(bc)b$ (B_{3g} symmetry) configurations. For the first one, the experimental spectrum was fitted with two damped oscillators [Fig. 4(a)] and for the other one with three damped oscillators [Fig. 4(b)]. In both configurations, the most intense mode (293.8 ± 0.1 cm^{-1} for A_g mode and 293.8 ± 0.1 cm^{-1} for B_{3g} mode) was considered as being a ν_1 mode because this breathing mode is usually expected to be the most intense.[33] Then the other observed modes were assigned as ν_3 modes [Fig. 4(b)].

In the $c(aa)b$ scattering geometry, three A_g modes are active but only two are observed. The 301.4 ± 0.1 cm^{-1} mode was logically assigned as one of the two ν_3 modes. The absence of observation of a second ν_3 mode can be due

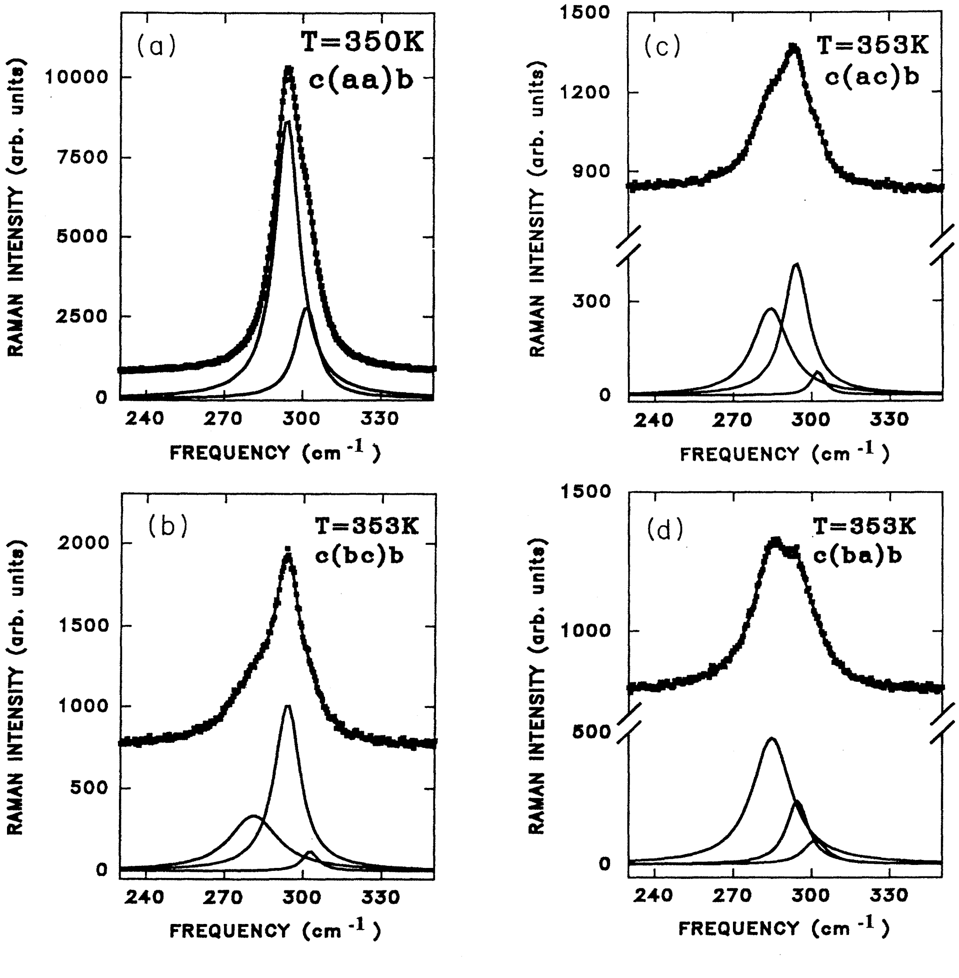

FIG. 4. Raman spectra of the stretching modes of Rb_2ZnCl_4 in the N phase. Filled squares represent the experimental data and the lines correspond to the overall calculated spectrum and deconvoluted individual modes. (a) in A_g symmetry, (b) in B_{3g} symmetry, (c) in B_{1g} symmetry, (d) in B_{2g} symmetry.

TABLE III. Slopes of the temperature dependence of the different A_g modes observed in the *INC* phase.

ν (cm^{-1})	285.0	294.0	302.3
$\partial\nu/\partial T$ (cm^{-1}/K)	-0.0169 ±0.0001	-0.0146 ±0.0001	-0.0265 ±0.0001

to an accidental degeneracy or to a very weak activity of the corresponding component of the polarizability tensor, as previously found in K_2SeO_4.[39] In the $c(bc)b$ scattering geometry, the two modes (281.1 ± 0.4 cm^{-1} and 302.7 ± 0.3 cm^{-1}) were assigned to the two expected ν_3 modes [Fig. 4(b)].

For both the $c(ac)b$ and $c(ba)b$ scattering geometries (B_{1g} and B_{2g} symmetries, respectively) a correct fit of the experimental spectra in the *N* phase definitely required three modes [Fig. 4(c) and 4(d)], whereas only one ν_3 stretching mode is expected in the hypothesis of a strict *Pmcn* symmetry (Table III). The unambiguous separation of several maxima was possible owing to the quality of the spectra that were recorded with a very high resolution and with a counting times sufficient for having good statistics (increment 0.2 cm^{-1} every 2 s). This allows us to see clearly several maxima on some spectra [Fig. 4(d)]. This anomaly constitutes an original result because, as explained in the following section, the observation of supplementary modes seems to correspond to an orientational disorder of the tetrahedra preceding the apparition of the modulation.

B. Interpretation and mode assignment

The interpretation of the existence of extra Raman lines not predicted by group theory rests on the hypothesis of a symmetry breaking due to an orientational disorder of the chlorozincate tetrahedra in the *N* phase. This type of behavior is similar to that suggested to exist for the anions of other compounds such as K_2SeO_4.[39]

The explanation is as follows. The condition specifying the apparition of one B_{1g} mode (or one B_{2g} mode), and only one, is based on the hypothesis of an ordered crystal. In Rb_2ZnCl_4, the origin of the second and third lines in the $c(ba)b$ and $c(ac)b$ scattering geometries can be interpreted, in agreement with Itoh's x-ray analysis,[19] as arising from a disorder in the tetrahedron orientations. The position in the mirror plane of the $\mathscr{D}_{2h}$ symmetry is unstable and the potential exhibits actually a double well about this position. Strict $\mathscr{D}_{2h}$ symmetry is lost though it remains an underlying average one. More precisely, the Cl atoms in position (1) and (2) (Fig. 5), which would be required to stay in the mirror plane $z=1/4$ in *Pmcn* symmetry, take randomly but with equal probability two possible positions out of the plane, the Cl atoms passing from one position to another through a rotation around the pseudohexagonal *c* axis.

The main consequence of this phenomenon is a breakdown of the selection rule validity for the ordered crystal and certain normally forbidden modes are then allowed to appear. Thus, in this case, the m_x mirror plane symmetry does not stand any more, so that the symmetric/antisymmetric behavior of the modes relative to this plane looses the strict meaning it had in the pure *Pmcn* structure: the antisymmetric modes acquire a slight symmetric character, and vice-versa. The previously denoted *u* (ungerade) modes become more or less weakly active in Raman-scattering spectra and their occurrence is then perceived as an anomaly from the point of view of the *Pmcn* mean structure. Consequently, in addition to the normally expected B_{1g} and B_{2g} modes (one ν_3'' frequency mode), B_{2u} and B_{1u} modes (more precisely predominantly B_{2u} and B_{1u} modes with a minor active symmetry *g* component) become possibly observable; note that these forbidden B_{2u} and B_{1u} modes must have a ν_3 or (and) ν_3' frequency since the modes of ν_1 frequency must be symmetric (*g*). Such extra lines have been previously reported by Massa, Ullmann, and Hardy[39] in their Raman spectra of the normal phase of K_2SeO_4. It is worthwhile noticing no such anomaly has been observed for external modes.[8,12]

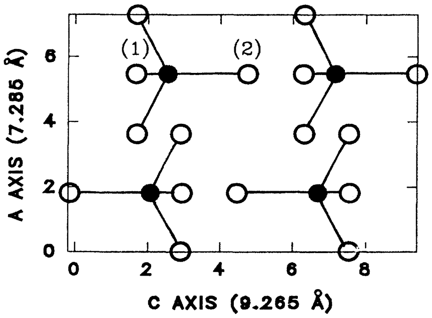

FIG. 5. Idealized representation of the $ZnCl_4$ tetrahedra projected onto the *ac* plane. Black circles: Zn; Open circles: Cl.

In view of this, we suggest the following assignments (Table IV) for the modes observed in the $c(ac)b$ and $c(ba)b$ scattering geometries: by analogy with the other polarizations, the mode at 293.9 cm^{-1} is assigned as the ν_1 breathing mode; and so the least intense mode at about 301.7 cm^{-1} and the mode at 281.1 cm^{-1} are two ν_3 modes. Thus the modes at 293.9 and 284.3 cm^{-1} (weak intensity) are two of those forbidden modes induced by the disorder as discussed above, i.e., a ν_1 mode and a ν_3 (or ν_3') one that would have had the B_{2u} (and B_{1u}, respectively) symmetry in a strict *Pmcn* structure. Care was especially taken in the experimental setup to eliminate the possibility that the forbid-

TABLE IV. Observed internal mode frequencies of Rb_2ZnCl_4 for the different symmetries in the normal phase ($T=353$ K).

Irreducible representation	Polarization	Frequency (cm^{-1})			
A_g	*aa*			293.8 ±0.1	301.4 ±0.1
B_{3g}	*bc*	281.1 ±0.3		293.8 ±0.1	302.0 ±0.3
B_{1g} (B_{2u})	*ab*		284.5 ±0.2	294.1 ±0.2	301.3 ±0.7
B_{2g} (B_{1u})	*ac*		284.2 ±0.2	294.0 ±0.1	302.1 ±0.2
Average frequency		281.1	284.3	293.9	301.7

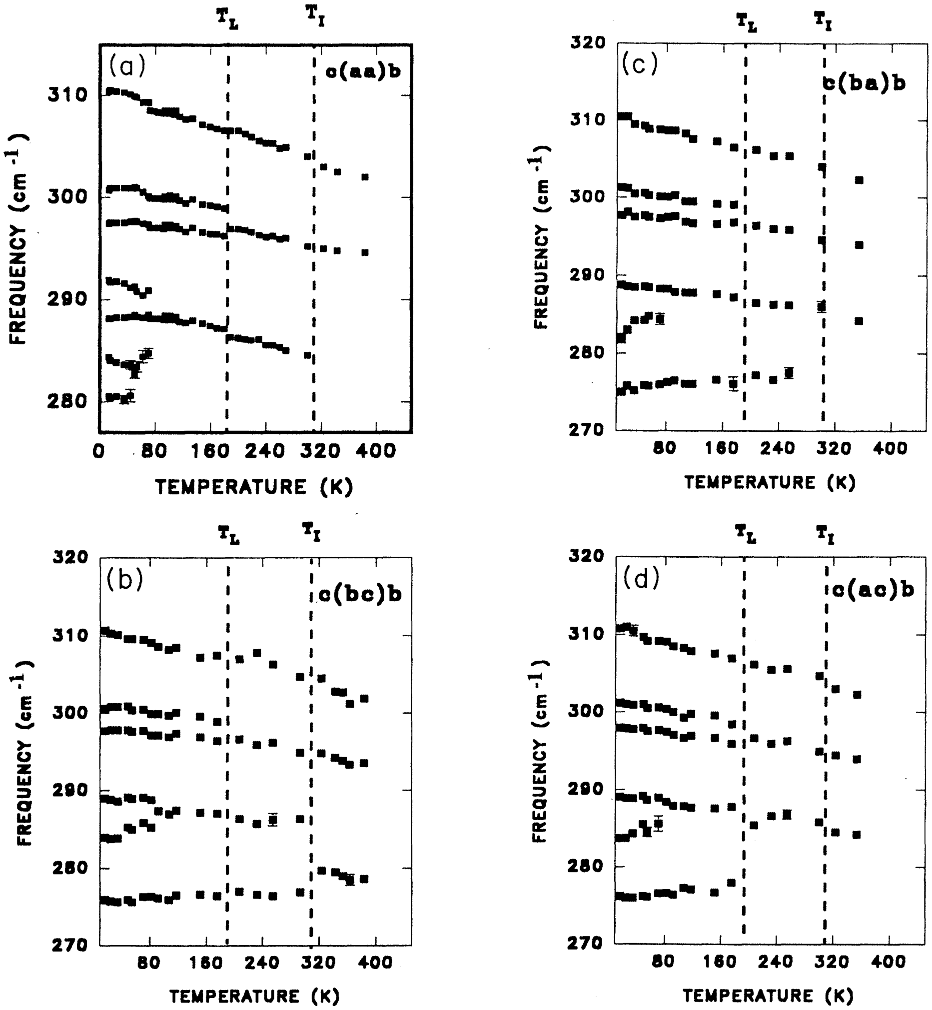

FIG. 6. Temperature dependence of the frequency of the modes observed. (a) in the $c(aa)b$ scattering geometry, (b) in the $c(bc)b$ scattering geometry, (c) in the $c(ba)b$ scattering geometry, (d) in the $c(ac)b$ scattering geometry.

den lines, i.e., those assigned to symmetry breaking could be an artifact corresponding to crystal misalignment or polarization leaks.

V. RAMAN SCATTERING SPECTRA IN THE INCOMMENSURATE AND COMMENSURATE PHASES

As the crystal undergoes the phase transition from the *N* phase to the *INC* phase at $T_I = 302$ K, the appearance of the modulation is revealed through the occurrence of extra modes at 285.0 ± 0.2 cm^{-1} (285.8 ± 0.3 cm^{-1}) in the A_g (B_{3g}, respectively) symmetry [Figs. 6(a) and 6(b)] and at 277.5 ± 0.4 cm^{-1} in the $c(ba)b$ scattering geometry [Fig. 6(c)]. The intensity of the 285.0 and 285.8 cm^{-1} mode, weak at 302 K (Fig. 7), increases continuously when the temperature decreases in the *INC* phase. The frequencies of the three A_g modes and the four B_{3g} modes vary as functions of temperature (Tables III and V, respectively).

In the $c(ac)b$ scattering geometry no supplementary mode is observed [Fig. 6(d)]. The anharmonicity of the three active modes already observed in the *N* phase can be at the origin of the lack of observation of supplementary modes. The linewidth of the breathing mode (293.9 cm^{-1}) is 5.5 cm^{-1} and that of the 302.1 cm^{-1} mode is equal to 3.2 cm^{-1}, while that of the 284.2 cm^{-1} mode is larger, around 9.3 cm^{-1}.

The strong temperature dependence of the internal mode frequencies indicates that these modes are affected by the modulation corresponding to the tetrahedron configuration disorder. Such a behavior has been interpreted by Rasing *et al.*[40] using modulated force constants. As commonly found in these kinds of compounds, the number of stretching modes effectively observed in all the experimental configurations is smaller than that predicted by (3+1) dimension group theory. This could be connected with a low modulated displacement of the Zn atoms and Cl atoms.[24] The extra-activated modes, resulting from phenomena rather weak, could not be observed by Raman scattering.

In the four scattering geometries, the *INC*-*C* phase transition at $T_L = 189$ K is revealed through a ν_1 mode splitting and a breaking in the slope of the temperature dependences of the frequencies. Only one mode appears in the $c(ac)b$ scattering geometry. These observations can be interpreted by a different description of the *INC* phase and *C* phase. In the *INC* phase the modulation corresponds to a continuum of tetrahedron orientations, while in the *C* phase it is characterized by only three tetrahedron configurations. Moreover the

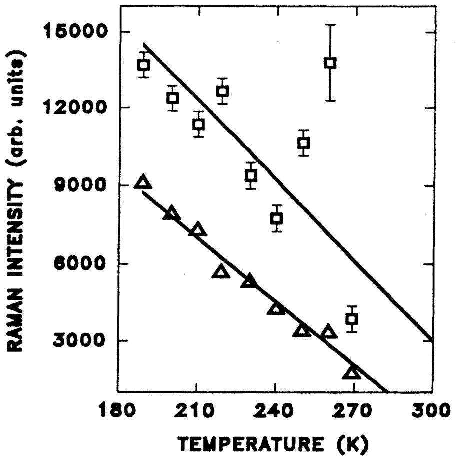

FIG. 7. Integrated intensity of the 285 cm^{-1} mode as a function of the temperature in the *INC* phase in the A_g (△) and B_{3g} (□) symmetries. Lines are a guide for the eyes.

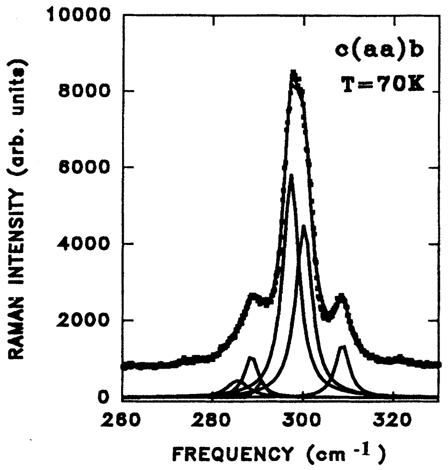

FIG. 8. Raman spectra of the stretching modes of Rb_2ZnCl_4 in a symmetrical scattering geometry at 70 K. Filled squares represent the experimental data and the lines correspond to the overall calculated spectrum and deconvoluted individual modes.

lowering in the symmetry removes degeneracies so that additional modes become active in the *C* phase which is predicted through a group theory analysis. In view of this, the orientational disorder in the *N* phase can be looked at as a precursor of the *INC* modulation that appears at T_I and finally becomes locked at T_L.

VI. RAMAN SPECTRA AT LOW TEMPERATURE

In the $c(aa)b$ scattering geometry, rather weak slope breakings are observed in the temperature dependence of the 297.4, 300.2, and 309.1 cm^{-1} mode frequencies at $T_1 = 80$ K [Fig. 6(a)]. Moreover supplementary modes that seem to arise from the splitting of the 288.4 cm^{-1} mode are also observed at this temperature. These modes are accurately defined by the fitting of the spectra below 80 K though with some asymmetry. This means that the supplementary modes appear very progressively as temperature decreases. It follows that establishing with precision a temperature phase transition via Raman scattering is quite difficult considering the spreading of this phenomenon versus temperature and the weak intensity of the observed modes (Fig. 8). At lower temperature, near 50 K, the spectrum seems to be modified. New modes and a breaking in the slopes of the temperature dependences of the frequencies are observed. Although these phenomena take place on some modes with relatively weak intensity, no doubt subsists about the presence of a new transformation or a new phase transition.

For the other three scattering orientations, slope breakings of the same modes are observed at 80 K ($\cong T_1$). Here also an asymmetry is clearly visible in the spectrum from 90 K downwards. At lower temperature, it is really too difficult to observe similar features as for the $c(aa)b$ configuration because of the too low intensity and the poor definition of the spectra. We assign the different rates for the frequency temperature dependences of the modes around 80 and 50 K, for all polarizations, to structural modifications most likely correlated with tetrahedron arrangements at both these temperatures. These successive modifications could be two different manifestations of a single phenomenon that would take place over a wide range of temperature in a slow and diffuse way. Since anomalies concern the internal modes, this phenomenon could be thought as consisting of a progressive rearrangement of the tetrahedra. Raman-scattering experiments, carried out by Francke *et al.*[41] relating to the external modes, complete this interpretation. In the $a(ca)b$ configuration, these authors observe, below 90 K, a rather weak mode that grows close to the Rayleigh line; this mode is well defined at around 80 K and they assign it to the pseudophase mode because of the strong variation of its frequency against temperature. Moreover, in the $a(cc)b$ configuration, they observe a low-frequency mode below 77 K; between 47 and 64 K, its frequency temperature dependence is described by a $(T_1 - T)^{2\beta}$ law with $2\beta = 1/2$ and $T_1 = 75$ K. This mode remains underdamped at T_1, which is an unusual behavior for a soft mode. In the same region of temperature, Gûnter *et al.*[31] have pointed out small dielectric anomalies at 75 K and Unruh and Stromich[30] have detected a spontaneous polarization along the pseudohexagonal **c** axis in addition to that known along the polar axis of the *C* phase. Specific measurements by Chaudhuri *et al.*[42] are also in favor of a phase transition around 75 K. Their thermograms exhibit the fairly diffuse and weak energy nature of this transition since it extends over the whole 75–50 K region.

VII. CONCLUSION

The temperature dependencies of the frequencies of the internal vibrational modes in Rb_2ZnCl_4 determined by Raman scattering and measured between 400 and 15 K make evident the *N-INC* phase transition and the *INC-C* phase transition. This measurement technique clearly reveals that Rb_2ZnCl_4 possesses an orientational disorder of the chlorozincate groups. Several hypothesis could be held to explain such a disorder.

The first one should take into account that the crystallization of Rb_2ZnCl_4 through slow evaporation at room temperature induces intrinsic defects. This influences the Raman

TABLE V. Slopes of the temperature dependence of the different B_{3g} modes observed in the *INC* phase.

ν (cm^{-1})	276.4	285.8	294.0	305.1
$\partial\nu/\partial T$ (cm^{-1}/K)	-0.0008 ± 0.0001	-0.0019 ± 0.0001	-0.0181 ± 0.0001	-0.0061 ± 0.0001

spectra, particularly those of the internal modes. The forbidden modes that appear in the normal phase could eventually be associated with these intrinsic defects[39] and that the freezing of the tetrahedra by the defects might induce supplementary modes.

The second hypothesis is directly connected by the appearance of supplementary modes for both B_{1g} and B_{2g} symmetries. Two modes not predicted by group theory have been observed by Raman scattering at 293.9 and 284.3 cm^{-1} frequencies. One can notice that the last one (284.3 cm^{-1}) corresponds to the frequency of the extra-activated mode observed in the *INC* phase. In this one, the 284.3 cm^{-1} mode is directly connected by the appearance of the modulation which indicates a long-wavelength disorder of the tetrahedra. So in connection with this result, we could argue that the 284.3 cm^{-1} mode observed in the *N* phase has the same origin. It corresponds to a local disorder of the tetrahedra. This disorder destroys the center of symmetry that should be present in the *N* phase. It can be looked at as a precursor of the modulation that appears at T_I. Such a behavior has been observed in an isomorphous compound, K_2SeO_4: more internal mode Raman lines than those that are predicted by *Pmcn* group theory were also found. In both cases, these crystals were grown by slow evaporation of aqueous solutions and so they are likely to contain intrinsic defects that could lock partly the orientation of the tetrahedral groups. The difference between these two compounds is that the disorder is less marked in the selenate due to a low rotation of the SeO_4^{2-} tetrahedra compared to those in $ZnCl_4^{2-}$ tetrahedra; this is consistent with the smaller frequency shifts among different symmetry components observed for the internal vibrational modes.[43] Moreover, molecular-dynamics simulations indicate that the double well in Rb_2ZnCl_4 is much deeper than in K_2SeO_4, thus causing the much more severe disorder in the *N* phase of Rb_2ZnCl_4.[44]

At low temperature Raman-scattering spectra clearly exhibit two phase transitions. The first one takes place at about 80 K and the second one at about 50 K. It is as yet too early to decide whether these two phenomena correspond to a unique slow and diffuse transformation as it is observed in K_2ZnCl_4 (Ref. 45) or to two different ones. By comparing these transformations with those of K_2ZnCl_4, it seems that the former result from the same phenomena but not so intense and not so spread in temperature. This could be interpreted by the fact that the amplitude of the modulation is more important in K_2ZnCl_4 than in Rb_2ZnCl_4.[24,36] However, it appears that these (or that) transformations are strongly correlated with the disorder observed in the *N* phase. The conditions of crystal growth could be at the origin first, of different phase transition sequences at lower temperature in these compounds and second, of orientational disorder of the tetrahedral groups in the *N* phase. Indeed, at room temperature, K_2SeO_4 grows in the *N* phase whereas Rb_2ZnCl_4 and K_2ZnCl_4 grow in the *INC* phase near T_I and in the $c^*/3$ superstructure phase, respectively. X-ray-diffraction experiments should be undertaken in order to learn more about the nature of these low-temperature phase transitions.

---

[1] H. Z. Cummins, Phys. Rep. **185**, 323 (1990).

[2] V. Dvorak and R. Kind, Phys. Status Solidi B **107**, 109 (1981).

[3] P. Muralt, E. Voit, and R. Kind, Phys. Status Solidi B **119**, 65 (1983).

[4] S. Sawada, Y. Shiroishi, A. Yamamoto, M. Takashige, and M. Matsuo, J. Phys. Soc. Jpn. **43**, 2099 (1977).

[5] A. Janner, Th. Rasing, P. Bennema, and W. H. v. d. Linden, Phys. Rev. **45**, 1700 (1980).

[6] E. Schneider and J. Petersson, Z. Phys. B **46**, 169 (1982).

[7] B. W. Van Beest, A. Janner, and R. Blinc, J. Phys. C **16**, 5409 (1983).

[8] M. Wada, A. Sawada, and Y. Ishibashi, J. Phys. Soc. Jpn. **47**, 1185 (1979).

[9] A. Gibaud, S. M. Shapiro, and J. Y. Gesland, J. Phys. Condens. Matter **3**, 4817 (1991).

[10] A. K. Moskalev, I. A. Belobrova, and I. P. Aleksandrova, Sov. Phys. Solid State **20**, 1896 (1978).

[11] M. Wada, A. Sawada, Y. Ishibashi, and Y. Takagi, J. Phys. Soc. Jpn. **42**, 1229 (1977).

[12] M. Wada, A. Sawada, and Y. Ishibashi, J. Phys. Soc. Jpn. **45**, 1429 (1978).

[13] R. Blinc, S. Juznic, V. Rutar, J. Seliger, and S. Zumer, Phys. Rev. **44**, 609 (1980).

[14] R. Osredkar, S. Juznic, V. Rutar, J. Seliger, and R. Blinc, Ferroelectrics **24**, 147 (1980).

[15] S. Hirotsu, K. Toyota, and K. Hamano, J. Phys. Soc. Jpn. **46**, 1389 (1979).

[16] C. J. De Pater and C. Van Dijk, Phys. Rev. B **18**, 1281 (1978).

[17] C. J. De Pater, Acta Crystallogr. B **35**, 299 (1979).

[18] H. Matsunaga, J. Phys. Soc. Jpn. **51**, 873 (1982).

[19] K. Itoh, A. Hinasada, H. Matsunaga, and E. Nakamura, J. Phys. Soc. Jpn. **52**, 664 (1983).

[20] M. Quilichini and J. Pannetier, Acta Crystallogr. B **39**, 657 (1983).

[21] K. Gesi and M. Iizumi, J. Phys. Soc. Jpn. **46**, 697 (1979).

[22] S. R. Andrews and H. Mashiyama, J. Phys. C **16**, 4985 (1983).

[23] H. Mashiyama, S. Tanisaki, and K. Hamono, J. Phys. Soc. Jpn. **51**, 2538 (1982).

[24] A. Hedoux, D. Grebille, J. Jaud, and G. Godefroy, Acta Crystallogr. B **45**, 370 (1989).

[25] H. Mashiyama, S. Tanisaki, and K. Hamono, J. Phys. Soc. Jpn. **50**, 2139 (1980).

[26] A. Hedoux, D. Grebille, J. Lefebvre, and R. Perret, Phase Transitions **14**, 177 (1989).

[27] J. Fousek, J. Kroupa, and J. Chapelle, Solid State Commun. **63**, 769 (1987).

[28] K. Hamano, Y. Ikeda, T. Fuimoto, K. Ema, and S. Hirotsu, J. Phys. Soc. Jpn. **49**, 2278 (1980).

[29] K. Hamano, in *Incommensurate Phases in Dielectrics*, edited by

R. Blinc and A. P. Levanyuck (North-Holland, Amsterdam, 1986).

[30] H. G. Unruh and J. Strômich, Solid State Commun. **39**, 737 (1981).

[31] P. Gûnther, R. Santuary, F. Rohner, H. Arend, and W. Seidenbusch, Solid State Commun. **37**, 883 (1981).

[32] A. Hedoux, I. Noiret, Y. Guinet, G. Odou, and J. Lefebvre, J. Chem. Phys. **97**, 6181 (1992).

[33] V. Katkanant, F. G. Ullman, and J. R. Hardy, Jpn. J. Appl. Phys. **24**, 790 (1985).

[34] A. S. Davydov, *Theory of Molecular Excitons* (McGraw-Hill, New York, 1962).

[35] H. Mashiyama, J. Phys. Soc. Jpn. **50**, 2655 (1981).

[36] M. Quilichini, P. Bernede, J. Lefebvre, and P. Schweiss, J. Phys. Condens. Matter **2**, 4543 (1990).

[37] K. Gesi and M. Iizumi, J. Phys. Soc. Jpn. **53**, 4271 (1984).

[38] I. Noiret, Ph.D. thesis, Lille 1, France, 1994.

[39] N. E. Massa, F. G. Ullman, and J. R. Hardy, Phys. Rev. B **27**, 1523 (1983).

[40] Th. Rasing, P. Wyder, A. Janner, and T. Janssen, Phys. Rev. B **25**, 7504 (1982).

[41] F. Francke, M. Le Postollec, J. P. Mathieu, and H. Poulet, Solid State Commun. **33**, 155 (1980).

[42] B. K. Chaudhuri, K. Nomoto, T. Atake, and H. Chihara, Phys. Lett. **79**, 361 (1980).

[43] V. Katkanant, J. R. Hardy, and F. G. Ullman, Ferroelectrics **82**, 185 1988.

[44] H. M. Lu and J. R. Hardy, Phys. Rev. B **45**, 7609 (1992).

[45] I. Noiret, A. Hedoux, Y. Guinet, and M. Foulon, Europhys. Lett. **22**, 265 (1993).